Third flight of the CREAM instrument

A. Putze[a,1], H. S. Ahn[2], T. Anderson[4], L. Barbier[5], A. Barrau[1], R. Bazer-Bachi[7], J. J. Beatty[8], P. Bhoyar[2], T. J. Brandt[8], M. Buénerd[1], N. B. Conklin[4], S. Coutu[4], L. Derome[1], M. A. DuVernois[9], O. Ganel[2], M. Geske[4], J. H. Han[2], J. A. Jeon[10], K. C. Kim[2], M. H. Lee[2], J. T. Link[5,6], A. Malinin[2], M. Mangin-Brinet[1], A. Menchaca-Rocha[11], J. W. Mitchell[5], S. I. Mognet[4], G. Na[10], S. Nam[10], S. Nutter[12], I. H. Park[10], N. H. Park[10], J. N. Périé[**], Y. Sallaz-Damaz[*], E. S. Seo[†‡], P. Walpole[†], J. Wu[†], J. Yang[10], J. H. Yoo[†], Y. S. Yoon[2,3]

***Abstract*— The balloon-borne Cosmic Ray Energetics And Mass (CREAM) experiment investigates high energy cosmic rays (CRs) from 10^{12} eV to 10^{15} eV over the elemental range from protons to iron. CREAM extends direct measurements of cosmic-ray composition to energies where ground-based air shower detections are possible, thereby providing calibration for indirect measurements. The precise measurement of CRs in this energy range allows also to study the production (injection and acceleration) and propagation processes in the Galaxy. A third flight of $\sim$ 29 days was accomplished in the Antarctic Summer 07/08, resulting in an overall accumulation of almost 100 days of exposure for the CREAM payload. Elemental spectra of cosmic ray particles for $1 \leq Z \leq 26$ were measured at the top of atmosphere with excellent charge and energy resolution, assured respectively by a Silicon Charge Detector (SCD) and a Cherenkov Imager (CherCam) for the charge and a tungsten-scintillator fiber ionisation calorimeter for the energy measurements. The instrument performance during this flight and results from the on-going data analysis, particulary for the CherCam detector for which it was the first flight, are presented.**

I. Introduction

The production and acceleration sites of galactic cosmic rays are presently unknown, even though there is evidence pointing to supernova remnants as natural acceleration site candidates [2], [4]. Cosmic rays originating from these sources diffuse through the Galaxy and may be confined by the galactic magnetic field. In addition, during galactic propagation, the cosmic-ray ions interact with the interstellar matter and produce secondary particles through nuclear fragmentation.

The goals of this project included the direct measurement of the energy spectra of primary cosmic rays and of their elemental composition up to the highest energies attainable in practice. The ultimate aim is to understand the mechanism of acceleration of primary cosmic rays up to very high energy, to identify their sources, and to clarify their interactions with the intergalactic medium. Since the discovery of cosmic rays nearly one hundred years ago, experiments to detect them directly have constantly improved. Today they are highly diversified to address different cosmic-ray processes over a wide energy range.

The spectral index of the energy spectra of the various elements comprising the cosmic-ray flux reflects the dynamics of their propagation, in particular the convolution of cosmic-ray source spectrum effects and those related to their propagation (acceleration, absorption, and escape). The evolution of the spectral index with the particle energy provides a sensitive test of the propagation processes determining that evolution. The precise measurement of the elemental abundances in the cosmic-ray flux, and in particular of the so-called secondary-to-primary ratios (e.g. B/C or subFe/Fe) leads to strong constraints on the galactic propagation models, because it is directly dependent on the total amount of material encountered by the particles during their propagation. The elucidation of particle propagation details in turn leads to a determination of the cosmic-ray source spectrum, and therefore to constraints on the acceleration processes.

The Cosmic Ray Energetics And Mass (CREAM) balloon-borne experiment measures the cosmic-ray spectrum of nuclear elements from proton to iron between 10^{12} eV and up to 10^{15} eV. This upper energy represents the statistical limit accessible to the current generation of balloon experiments, but also the lower threshold energy of ground-based indirect measurements of the cosmic-ray flux. Direct measurements of the elemental composition at these energies not only provide new data on cosmic-ray spectral characteristics and abundances but also serve as a calibration for the ground-based experiments, where data analysis is based on hadronic interaction models (such as QGSJET and SIBYLL), which can lead to different and sometimes inconsistent results.

The CREAM instrument measures simultaneously the relative abundances of secondary cosmic rays and the energy

[1]Laboratoire de Physique Subatomique et de Cosmologie LPSC, Grenoble, 38026, France
[2]Institute for Physical Science and Technology, University of Maryland, College Park, MD 20742, USA
[3]Department of Physics, University of Maryland, College Park, MD 20742, USA
[4]Department of Physics, Penn State University, University Park, PA 16802, USA
[5]Astrophysics Space Division, NASA Goddard Space Flight Center, Greenbelt, MD 20771, USA
[6]CRESST/USRA, Columbia, MD 21044
[7]Centre d'Etude Spatiale des Rayonnements, UFR PCA-CNRS-UPR 8002, Toulouse, France
[8]Department of Physics, Ohio State University, Columbus, OH 43210, USA
[9]Department of Physics, University of Hawaii, Honolulu, Hawaii 96822, USA
[10]Department of Physics, Ewha Womans University, Seoul 120-750, Republic of Korea
[11]Instituto de Fisica, Universidad National Autónoma de México, Mexico
[12]Department of Physics, Northern Kentucky University, Highland Heights, KY 41099, USA
[a]Corresponding author: putze@lpsc.in2p3.fr

spectra of primary nuclei, with excellent charge and energy resolution. In order to accomplish such a challenging task, the instrument consists of complementary and redundant detectors for charge identification and energy measurements. To assure sufficient statistics for the low flux of high-energy particles, the CREAM instrument was designed and constructed to have a large geometry factor (acceptance) and to fulfill all the requirements for NASA's Long-Duration Balloon flights. A detailed description of the CREAM instrument can be found in [1].

II. Three successful Long-Duration Balloon Flights of CREAM

The first flight of the CREAM experiment was launched from Williams Field near McMurdo Station in Antarctica on 16 December 2004, and ended nearly 42 days later, after circumnavigating the South Pole three times and establishing a new record for Long-Duration Balloon flights. A second flight (CREAM-II) took place exactly one year after the launch of CREAM-I. This time the experiment circumnavigated the South Pole twice and landed 28 days later. CREAM-III was launched on 19 December 2007. A first circumnavigation around the Pole was completed in 15 days and the balloon flew directly over McMurdo station from where it could be seen. The second round described a nearly perfect circle, as can be seen in Fig. 1 (top), and ended on 17 January 2008 after approximately 29 days of flight. The float altitude of the balloon during this flight, shown in Fig. 1 (bottom), varied from 35.7 (lower solid line) to 39.9 km (upper solid line), with a mean value of 38.2 km (dotted line) which corresponds to an atmospheric overburden of around 3.9 g/cm^2. With this third flight, a cumulative exposure of about 100 days was achieved in about 4 years, exceeding those of all prior balloon experiments. Additionally, due to the acceptance and the high float altitude of the detector, CREAM collected more protons and high-charge particles up to iron than any other balloon-borne experiment so far [8].

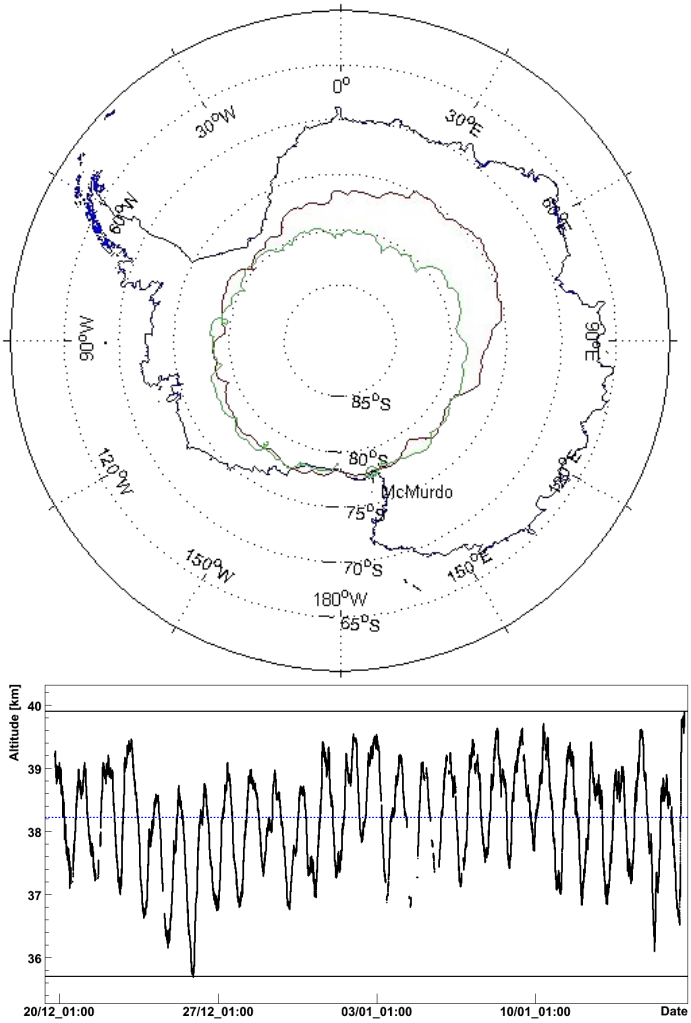

Fig. 1. Top: Balloon trajectory of the CREAM-III flight from 19 December 2007 to 17 January 2008. The outer red curve represents the first cricumnavigation and the inner green (nearly circular) curve the second circumnavigation. Bottom: Altitude of the CREAM-III experiment during this flight. The maximum (39.9 km, upper line), minimum (35.7 km, lower line), and mean altitude (38.2 km, dotted blue line) are represented.

III. The CREAM-III detector

The CREAM-III instrument consists of multiple charge and energy detectors (see Fig. 2 for an exploded view).

The Timing Charge Detector (TCD) is placed at the top of the instrument. This charge detector is made up of two crossed layers of large-area thin scintillator paddles read out via fast, low-jitter photomultiplier tubes. The Cherenkov Detector (CD), measures the Cherenkov radiation produced only by relativistic particles, with a 1 cm thick scintillator, and thus vetoes low-energy background particles. The CD is mounted directly on the Cherenkov Camera (CherCam), a proximity focusing Cherenkov imager. Detailed features of this subdetector, for which this was the first flight, will be discussed later in section IV. The double layer Silicon Charge Detector (SCD) is segmented into small pixels (2.12 cm^2) to minimise hits of accompanying back-scattered particles in the same segment as the incident particle. Two 9.5 cm thick carbon targets ($\rho = 1.92\,\mathrm{g/cm^3}$) with a 30° flare angle are mounted over the calorimeter, inducing nuclear interactions, allowing the calorimeter to measure incident energy through the resulting showers and to provide tracking information on the incident particle. The calorimeter is a sampling tungsten/scintillating fiber device, with 20 tungsten plates, each followed by a layer of $0.5\,\mathrm{mm}$ diameter scintillating fibers, arranged in 50 ribbons and comprised of 19 fibers each. To further reduce uncertainty due to back-scattering, a layer of $2 \times 2\,\mathrm{mm}^2$ scintillating fibers is positioned directly above the calorimeter stack. This detector, labeled S3, measures the time at which back-scattered particles start their way back to the TCD. One can then calculate the time at which the primary particle would have traversed the TCD scintillators, with an accuracy of better than 0.1 ns.

A more detailed description of the instrument can be found

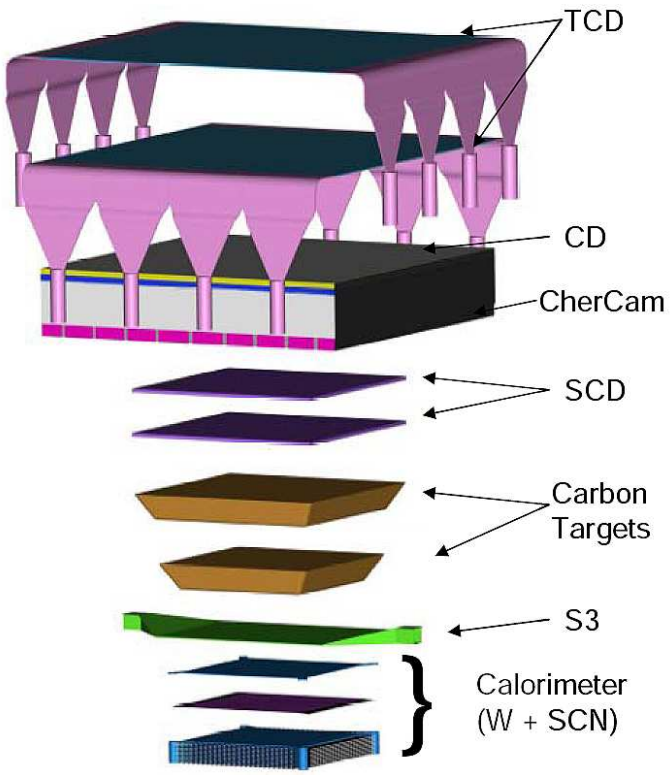

Fig. 2. Expanded view of the CREAM-III instrument

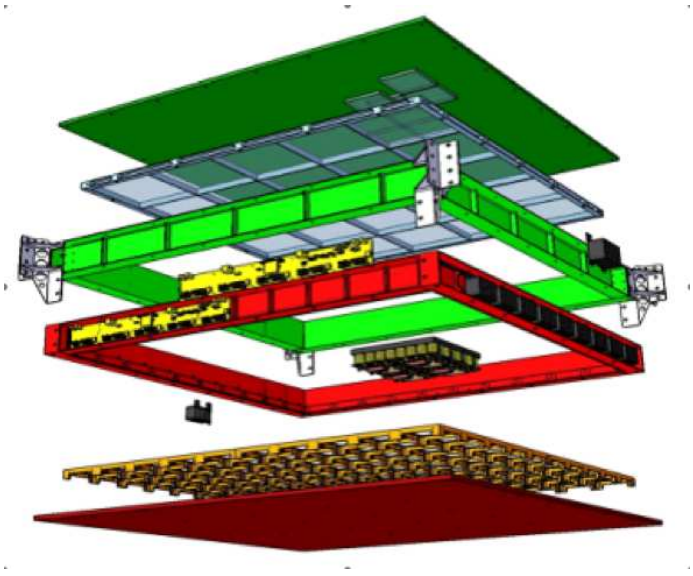

Fig. 3. Exploded CAD view of the CherCam mechanical structure

in [1].

IV. CherCam, a Cherenkov imager for CREAM [7]

A. CherCam design and architecture

The CherCam is a proximity focusing imager derived from the solution developed for the AMS experiment [3]. The detector is optimised for charge measurements, with a constant resolution through the range of nuclear charge from hydrogen to iron.

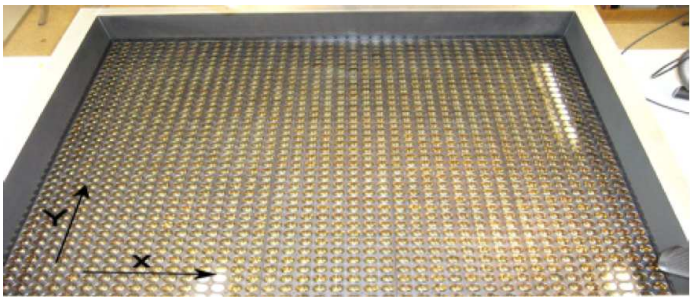

Fig. 4. Photomultiplier plane of CherCam composed of 1600 (40×40) 1 inch Photonis XP3112 photomultiplier tubes.

The Cherenkov radiator consists of a 20.8 mm thick silica aerogel plane, made of two superimposed layers of $10.5 \times 10.5\,\mathrm{cm}^2$ Matsushita-Panasonic SP50 tiles, with a refraction index $n \sim 1.05$. The radiator plane is separated from the photon detector plane by a 110.5 mm gap. The detector plane consists of an array of 1600 photomultiplier tubes (PMT, 1 inch Photonis XP3112), backed with custom dedicated front-end electronics, power supply, and readout electronics.

The mechanical structure of the detector is illustrated in Fig. 3. The upper frame includes the radiator plane fixed to the top lid, and an (empty) drift space. The lower frame supports the PMT array and the first level readout electronics.

PMTs are arranged in a square pattern with a 27.5 mm pitch (Fig. 4). The matrix is divided into 10×10 square blocks, each block consisting of 16 PMTs. All the PMTs are inserted in a 15 mm thick housing block of black epoxy material (ertalyte). This arrangement provides a photon detection active surface of about 50%. A light guide option had been studied to minimise the dead-space, but the reconstruction algorithm proved to be more efficient without the complex reflections introduced by guides. Each block is readout by the same 16-channel front-end ASIC as developed for the AMS Cherenkov imager, and is powered by a single dedicated high-voltage module. The 100 high-voltage modules were designed and built at LPSC Grenoble and CESR Toulouse. They are placed on two opposite external sides of the lower frame, while the data acquisition, housekeeping and control boards are fixed on the other two sides, respectively. The detector is also equipped with an LED light source coupled to an optical fiber array, used for single photon calibrations.

B. CherCam thermal, vacuum and beam tests

The CherCam has to operate under physical conditions close to space experiments with only radiative thermal dissipation, a low pressure environment and large temperature excursions. We successfully carried out a complete validation of the instrument through dedicated thermal test (power switch-on at -10 °C, low range thermal variation (-10 °C, +10 °C), thermal cycling at atmospheric pressure between -10 °C and +35 °C) and vacuum exposure (long duration (23 h) test at 5 mbar pressure).

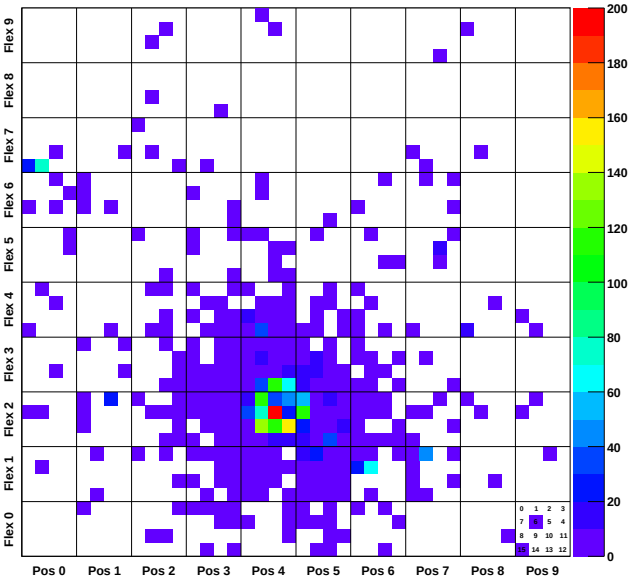

Fig. 5. High charge particle event in the CherCam. Each pixel represents one photomultiplier tube, where the color code indicates the number of Cherenkov photons seen. The Cherenkov ring and impact point of the incoming particle are clearly visible. The photons in the "halo" around the impact point are Rayleigh scattered photons.

A CherCam prototype had been tested in a secondary $Z = 1$ particle beam at CERN in October 2006 and 2007. The prototype consisted of a single 64 PMT module equipped with a partial set of flight electronics and a dedicated acquisition system for the beam test. The incident particle momentum used in the 2007 test ranged between 100 and 300 GeV/c. The $Z = 1$ particles provided a sensitive way of testing the background sources since the counter was operated at its lower limit of sensitivity. A preliminary estimate of the charge resolution gives a value of $\sigma_Z = 0.2$ charge units. This result is compatible with the expected performance and with the expectations derived from simulation studies.

V. CherCam event reconstruction

A. Constraints on the charge reconstruction

The principle of the CherCam detector is based on the detection of Cherenkov photons, emitted by an incoming high-energy particle passing through the radiator plane. A typical high charge particle event in the CherCam is represented in Fig. 5. The number of these emitted Cherenkov photons N_γ for a given wavelength range $\mathrm{d}\lambda$ is given by the Franck-Tamm formula, which, for $\beta = 1$, where β is the particle velocity in units of the speed of light (which is a good approximation given the energy of the particles measured by CREAM), and integrating over the path length in the radiator, reads:

$$\frac{\mathrm{d}N_\gamma}{\mathrm{d}\lambda} = 2\pi\alpha\frac{Z^2}{\lambda^2}\frac{d}{\cos\tau}\left(1 - \frac{1}{n(\lambda)^2}\right), \qquad (1)$$

where α is the fine structure constant ($\approx 1/137$), Z the particle charge, d the radiator thickness, τ the zenith angle of the incoming particle and n the refractive index of the radiator material. The number of emitted Cherenkov photons is proportional to the square of the incoming particle charge, hence allowing particle charge identification.

The number of Cherenkov photons detected by the CherCam $N_{\mathrm{det}}(x, y, \tau, \psi, Z)$ depends on the detection efficiency, which includes the quantum efficiency $\varepsilon_{\mathrm{QE}}$ of the photomultiplier tubes, and the geometrical efficiency $\varepsilon_{\mathrm{geo}}(x, y, \tau, \psi)$, defined as the detected-to-emitted photon ratio due to the CherCam architecture and Rayleigh scattering:

$$N_{\mathrm{det}}(x, y, \tau, \psi, Z) = \varepsilon_{\mathrm{geo}}(x, y, \tau, \psi) \cdot N_\gamma(\tau, Z), \qquad (2)$$

where

$$\begin{aligned} N_\gamma(\tau, Z) &= \int_{\lambda_{\min}}^{\lambda_{\max}} \varepsilon_{\mathrm{QE}}(\lambda) \cdot \frac{\mathrm{d}N_\gamma}{\mathrm{d}\lambda}\,\mathrm{d}\lambda \\ &= 2\pi\alpha Z^2 \frac{d}{\cos\tau}\int_{\lambda_{\min}}^{\lambda_{\max}} \left(1 - \frac{1}{n(\lambda)^2}\right)\frac{\varepsilon_{\mathrm{QE}}(\lambda)}{\lambda^2}\,\mathrm{d}\lambda \\ &= N_\gamma^{Z=1}\frac{Z^2}{\cos\tau}, \end{aligned} \qquad (3)$$

where $N_\gamma^{Z=1}$ represents the mean number of detected photons for a particle of charge $Z = 1$, a geometric efficiency $\varepsilon_{\mathrm{geo}} = 1$ and a normal incidence. Equation 2 then becomes

$$N_{\mathrm{det}}(x, y, \tau, \psi, Z) = \varepsilon_{\mathrm{geo}}(x, y, \tau, \psi) \cdot N_\gamma^{Z=1} \cdot \frac{Z^2}{\cos\tau}. \qquad (4)$$

N_{det} depends strongly, through the geometric efficiency $\varepsilon_{\mathrm{geo}}$, on the impact position (x, y) of the incoming particle on the radiator plane and its zenith and azimuth angles τ and ψ, respectively. Therefore, in order to assure the required precision of $\Delta Z < 0.3$ on the particle charge reconstruction up to iron ($Z = 26$), it is necessary to have a good knowledge of the particle trajectory. Indeed, based on the equation

$$\Delta Z = \frac{1}{2}\left(\frac{1}{\sqrt{N_{\mathrm{det}}^{Z=1}}} \oplus Z\frac{\Delta\varepsilon_{\mathrm{geo}}}{\varepsilon_{\mathrm{geo}}} \oplus Z\frac{\Delta\cos\tau}{\cos\tau}\right), \qquad (5)$$

the condition $\Delta Z < 0.3$ gives for $Z = 26$ and $N_{\mathrm{det}}^{Z=1} = 10$ an upper limit on $\sqrt{\left(\frac{\Delta\varepsilon_{\mathrm{geo}}}{\varepsilon_{\mathrm{geo}}}\right)^2 + \left(\frac{\Delta\cos\tau}{\cos\tau}\right)^2}$ of $2.3 \cdot 10^{-2}$. This number can be translated into a precision on the impact point (Δx and Δy), which must be known to within less than 1 mm for the two space directions [6].

B. Event reconstruction

As seen in section III the CREAM calorimeter yields a 3d track for the incoming particle. This leads to the identification of the region of interest within the multiple charge detectors of the CREAM-III instrument and provides for background noise for the charge measurement. Combining the knowledge of the track reconstructed in the calorimeter and of the impact points in the two layers of the SCD, the impact point within the CherCam detector can be extrapolated with good precision.

The calorimeter trigger needs 6 consecutive layers (3 in each plane) to be active. A layer is considered active if at least one ribbon's low-energy range (out of 50) registered a signal exceeding a commandable threshold, typically set at about 60 MeV [1]. To reconstruct the particle shower a clustering algorithm was used for each plane (X-Z and Y-Z), after pedestal correction and noise-channel subtraction. For each layer in a given plane the pixel with the maximum energy deposit and its closest neighbours within this cluster are used to calculate the center of gravity (COG) and the associated error (see Fig. 6 top panels).

For each layer (top and bottom) of the SCD a clustering algorithm is used, after pedestal correction and noise-channel subtraction, to find the impact point of the incoming particle. The pixel with the maximum signal within this cluster is identified as the pixel hit by the particle (see Fig. 6 middle panels). The two points are added to the ensemble of the resulting COG from the calorimeter event reconstruction. To extract the trace in the given plane the resulting ensemble of COGs and two SCD points is fitted linearly. The trajectory information (x, y, τ, ψ) is obtained by combining the fit results of the two spatial planes.

The resolution on the track reconstruction can be evaluated by using the CREAM calorimeter and SCD data extrapolated to the CherCam level. Figure 6 (bottom panels) shows the distribution of the difference between the extrapolated and reconstructed impact points (in the x and y directions, respectively) on the CherCam, where the reconstructed impact point corresponds to the pixel within the chosen cluster of hit PMTs with the maximum number of detected photons. A resolution of $\sim 11\,\mathrm{mm}$ is found, which is insufficient for the charge reconstruction accuracy required as described in the section above. Therefore it is necessary to add the CherCam event information to the track reconstruction.

For the event reconstruction in the CherCam an overlap method is used. The idea is to superpose a simulated event over the measured event and to minimise the following χ^2 with the help of a Powell algorithm [5]:

$$\chi^2 = \sum_{i}^{\text{PMT hit}} \frac{1}{n_i^{\text{det}}} \left(n_i^{\text{det}} - n_i^{\text{est}}(x, y, \tau, \psi)\right)^2, \qquad (6)$$

where n_i^{det} and n_i^{est} are the detected and estimated photon numbers in the hit PMT i, respectively.

A CherCam simulation package was developed [7], based on the GEANT4 toolkit, to provide simulated events and to investigate the detector response. In addition to the CherCam architecture (as described in section IV-A) simulation, it includes Cherenkov light generation in the radiator and its propagation (refraction and reflection), Rayleigh scattering dispersion and photon detection by modelised photomultipliers. The photocathode quantum efficiency is taken into acount according to the data provided by the PMT manufacturer. In Fig. 7 an incoming beryllium nucleus with normal incidence produces Cherenkov photons, represented by the green lines, in the radiator plane. After their travel through the detector they are detected in the photomultiplier plane below.

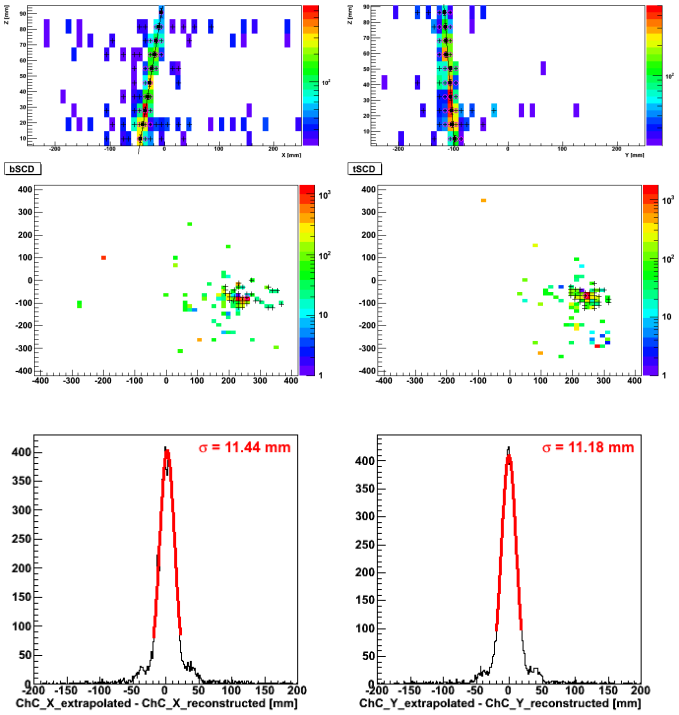

Fig. 6. Top panels: Event in the CREAM-III calorimeter. Represented are the X-Z (left) and the Y-Z plane (right), containing 50×10 ribbons for the energy and track reconstruction. The color code indicates the energy deposit in each ribbon. Ribbons marked with crosses are considered to be hit by the particle shower (cluster). The ribbon with the maximum energy deposit and its closest neighbours are identified. Such pixels with maximum activity are used to calculate the COG, permitting the reconstruction of the shower direction through a linear fit (black line). Middle panels: Event in the bottom (left) and top (right) SCD (51×55 pixels). The color code represents the energy deposit in each pixel. The pixel with the maximum energy deposit inside the cluster (crosses) is considered to be the pixel hit by the incoming particle. Bottom panels: Resolution of the impact point reconstruction in the x (left) and y directions (right). The tracking information from the calorimeter and the SCD is used to linearly extrapolate the impact point of the incident particle on the CherCam. The reconstructed impact point is the centre of the PMT entrance window with the maximum photon number in the cluster, considered to be hit by the incoming particle.

A second event simulation package was also developed, with a simpler detector geometry than in the GEANT4 version. This package provides, with minimal computing time, the number of estimated photons $n_i^{\text{est}}(x, y, \tau, \psi)$ in the PMT i, produced by an incoming particle (simulated) with a trajectory given by τ and ψ and an impact point (x, y) on the CherCam detector. The reconstruction of simulated event samples (overlap of two simulated events) shows that the charge reconstruction accuracy remains within $\Delta Z = 0.28$ over the whole charge range considered with this simulation package. The overlap fit also provides a more precise impact point on the CherCam detector than the PMT center ansatz, which was used for the prior track resolution evaluation. Figure 8 shows the improved evaluation using the reconstructed impact point of the overlap fit after minimisation. A $\sim 2\,\mathrm{mm}$ improvement on the track reconstruction resolution is thus achieved.

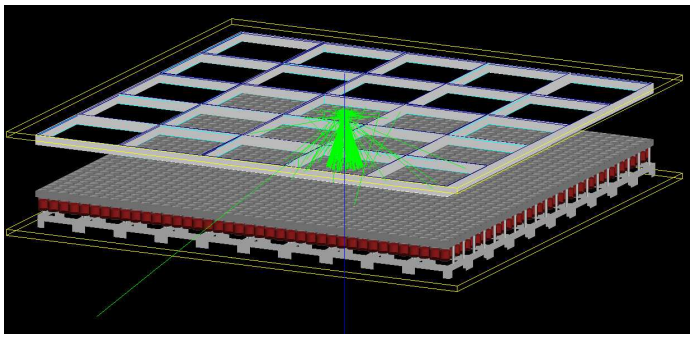

Fig. 7. GEANT4 simulation of the CherCam detector

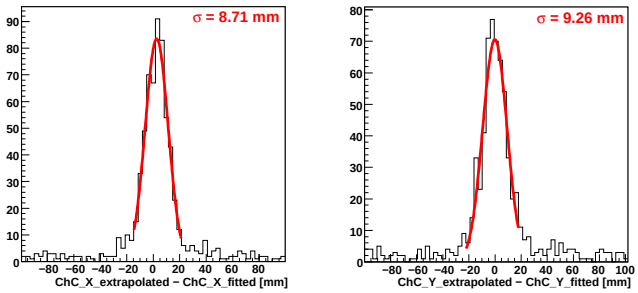

Fig. 8. Resolution of the impact point reconstruction in the x (left) and y directions (right). The calorimeter and SCD track is linearly extrapolated to find the impact point of the incident particle on the CherCam. The reconstructed impact point is the result of the overlap method described in the text.

VI. Conclusions and Perspectives

After two previous successful flights of the CREAM instrument, the detector accomplished a third during the Antartic summer 2007/2008. During the 29 day long flight, about 1.5×10^6 events were collected, achieving a cumulative flight exposure of about 100 days. This is the longest cumulative flight exposure of any previous balloon experiments and represents the largest event set so far. The CREAM-III instrument is composed of multiple charge and energy detectors, amongst them the CherCam, a Cherenkov imager, for which this was the first flight. The detector, measuring the incoming particle charge with a constant resolution from hydrogen to iron, was designed and fully integrated in less than two years, and tested in space-like conditions. The maximum charge resolution requires a good knowledge of the particle trajectory, which is determined by two other subdetectors of the CREAM instrument: the calorimeter and the SCD. The resulting resolution was found not to be sufficient, and an additionnal CherCam event fit, based on a overlap between a simulated and real event, was needed. Therefore two simulation packages were developed, in order to study the physical processes inside the detector and to develop a data analysis algorithm integrating the different phenomena. Preliminary results of the charge reconstruction of simulated events show that the desirec charge resolution is obtained over the whole charge range studied. The data analysis of the events collected during the flight is in progress.

In the meantime a fourth flight of CREAM is in preparation. The instrument will be launched in December 2008 with the CherCam on board.

References

[1] H. S. Ahn *et al*. *Nuclear Instruments and Methods in Physics Research A*, 579:1034–1053, 2007.

[2] V. S. Berezinskii, S. V. Bulanov, V. A. Dogiel, and V. S. Ptuskin. *Astrophysics of cosmic rays*. Amsterdam: North-Holland, edited by Ginzburg, V.L., 1990.

[3] L. Gallin-Martel *et al*. *Nuclear Instruments and Methods in Physics Research A*, 504:273–275, May 2003.

[4] M. S Longair. *High energy astrophysics - volume 1 (2nd ed)*. Cambridge University Press, 1992.

[5] W. H. Press, B. P. Flannery, and S. A. Teukolsky. *Numerical recipes. The art of scientific computing*. Cambridge: University Press, 1986.

[6] Y. Sallaz-Damaz. PhD thesis, Université Joseph Fourier, 2008.

[7] Y. Sallaz-Damaz *et al*. *Nuclear Instruments and Methods in Physics Research A*, 595:62–66, September 2008.

[8] E. S. Seo *et al*. *JPSP Supplements*, in print.